Gas-Phase Reactions of Nickel and Nickel Oxide Clusters with Nitrogen Oxides. 3. Reactions of Cations with Nitric Oxide

W. D. Vann, R. C. Bell, and A. W. Castleman, Jr.*

Department of Chemistry, Pennsylvania State University, 152 Davey Laboratory, University Park, Pennsylvania 16802

Received: August 16, 1999

A fast flow reactor−quadrupole mass spectrometer system coupled with a laser vaporization source is used to study the gas-phase reactions of nickel and nickel oxide cluster cations with nitric oxide. Pseudo-first-order bimolecular rate constants are reported for the reactions of NO with nickel and nickel oxide cluster cations and O_2 reactions with nickel cluster cations. The product distributions indicate that several different reaction mechanisms occur between NO and Ni_x^+ and $Ni_xO_y^+$. Competing processes such as oxidation, NO addition, and replacement of oxygen with nitric oxide are observed to occur. Also, the presence of magic peaks in the distributions indicates unusually stable product cluster species.

I. Introduction

The use of cluster chemistry allows intermediate reactions relevant to certain catalytic processes to be studied in the gas phase. Investigating reactions at flow tube pressures around 300 mTorr provides an intermediate pressure step between surface studies and actual catalytic processes. Cluster systems can function as molecular scale models of localized catalytic systems, and, through their use, short-range interactions between the catalyst and the reactants can be carefully investigated. Potential reaction mechanisms, reaction rates, competing reactions, and poisoning processes can be examined in detail through the use of cluster chemistry. Metal[1] and metal oxide[2] clusters are often used to provide useful information for interactions occurring between a catalyst and reactant. The work described in this paper is part of an ongoing investigation designed to understand these types of interactions between nickel and nickel oxide catalysts and NO_x gases.

Reactions of both nickel and nickel oxide anion clusters have been reported previously with nitric oxide, which formed, among other species, both nitrogen dioxides attached to the clusters and free nitrogen dioxide anions.[3,4] These reactions lead to some interesting insights into how electron density may effect local reaction centers in heterogeneous catalysts. The present paper focuses on gas-phase reactions of nickel and nickel oxide cluster cations ($Ni_xO_y^+$, where $x = 1-16$ and $y = 0-10$) with nitric oxide under well-defined thermal conditions.

To study these reactions, nickel clusters cations are produced by laser vaporization, reacted in a fast flow reactor, and then detected by a quadrupole mass spectrometer. This paper presents new information on reactions, reaction rates, and reaction mechanisms occurring between nickel and nickel oxide cluster cations and nitric oxide.

II. Experimental Section

The fast flow reactor mass spectrometer used in this work has been described in detail previously.[3−5] Briefly, a nickel rod is vaporized in the presence of a flowing stream of helium carrier gas. The continuous flow carries the ablation species out of the source through a conical nozzle into the flow tube. Laser vaporization is performed using the second harmonic of a Nd:YAG laser focused by a 20-cm focal length lens onto a 0.6-cm rotating nickel rod.

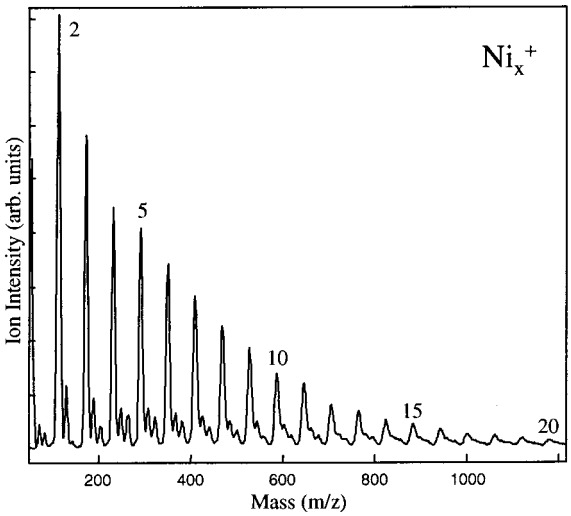

Figure 1. Typical nickel cluster cation distribution.

As the ions are carried through the flow tube, they are thermalized (296 K) by collisions with the carrier gas. The flow tube pressure is maintained at around 300 mTorr. Neutral reactant gases are added through a reactant gas inlet and are allowed to react with the cluster ions for a measured amount of time before they are sampled into a quadrupole mass filter and detected by a channel electron multiplier.

III. Results and Discussion

Nickel Cluster Cations. Both nickel and nickel oxide cluster cations are formed by laser vaporization of a nickel rod. Figure 1 shows a typical nickel cation cluster distribution with various peaks labeled as Ni_x^+. The spectrum shows nickel clusters to Ni_{20}^+. Clusters from Ni_{20}^+ to Ni_{30}^+ are also detected with this apparatus; however, their signal intensity is insufficient for experimental purposes. Also, a small amount of Ni_xO^+ and

10.1021/jp992893r CCC: $18.00
Published on Web 11/19/1999

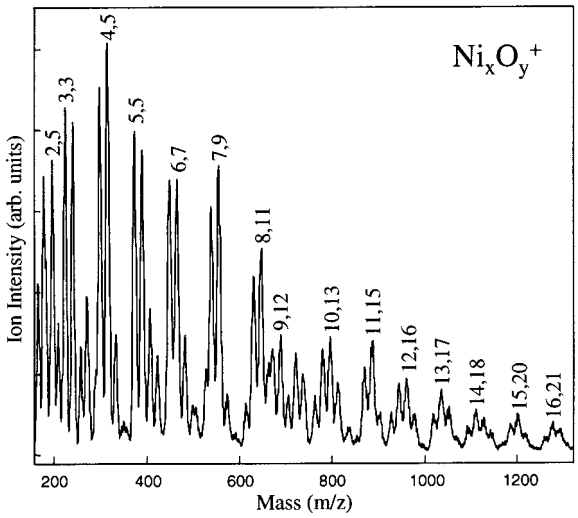

Figure 2. Typical nickel oxide cluster cation distribution.

$Ni_xO_2^+$ can be seen throughout the spectrum. These small amounts of oxides are from minute leakage of air into the laser vaporization source at the o-ring seal.

Nickel Oxide Cluster Cations. A nickel oxide cation cluster distribution is given in Figure 2. The major peaks in this spectrum are labeled as $Ni_xO_y^+$. This distribution shows nickel oxides from $Ni_2O_y^+$ to $Ni_{16}O_y^+$. These oxides were produced by flowing 20 mTorr of oxygen over the rod during laser vaporization. Nickel oxide cations are somewhat more difficult to saturate with oxygen than are anions. As much as 20 mTorr of oxygen was added to the laser vaporization source before saturation occurred. By contrast, anion saturation was achieved with as little as 1 mTorr of oxygen. It should be noted, however, that very little difference is achieved when going from 1 to 20 mTorr with cations. For instance, the $Ni_{15}O_{19}^+$ shifts to $Ni_{15}O_{20}^+$, the $Ni_9O_{10}^+$ to $Ni_9O_{12}^+$, and the $Ni_3O_4^+$ to $Ni_3O_6^+$.

As with nickel oxide anions,[3] the cation distribution shown in Figure 2 is affected by the preferred oxidation states of nickel. While exact oxidation states cannot be assigned without knowing the structure of the cluster, considering the possible oxidation states of the metals within the cluster gives some insight into the preferred cluster stoichiometry. If one were to assign oxidation states on the basis of the assumption that these oxide cluster are strongly bonded nonhomogeneous oxides, the majority of the nickel oxide clusters produced in both cation and anion experiments could be explained by a combination of stoichiometric nickel(II) and (III) oxides. The most common oxidation state for nickel is the divalent NiO.[6] However, trivalent nickel oxides, Ni_2O_3, are also known to be present at nickel surfaces.[7] The $Ni_3O_4^+$, NiO_2^-, and $Ni_3O_5^-$ are examples of cluster ions likely having a valence of III. Valence mixing of Ni(II) and Ni(III) is also known to occur in nickel oxides.[8] Mixed valence nickel oxide clusters could perhaps be better expressed in terms of less localized electrons, where the oxidation state is given as a noninteger value. On the basis of the fact that divalent and trivalent complexes are most common with nickel,[6,7,9] it is reasonable to expect that oxidation states would all be around II to III. This is consistent with what is observed experimentally for both cations and anions of nickel oxides as well as other metals.[10] From $Ni_4O_4^+$ (2.25) to $Ni_{16}O_{22}^+$ (2.8), the mixed valence oxidation states of these nickel oxide clusters are all between 2.25 and 2.8. Larger nickel oxide clusters observed experimentally such as $Ni_{17}O_{23}^+$, $Ni_{18}O_{24}^+$, $Ni_{19}O_{26}^+$, $Ni_2O_{26}^+$, $Ni_{21}O_{27}^+$, $Ni_{22}O_{29}^+$, and $Ni_{23}O_{29}^+$ also have mixed valence oxidation states between 2.6 and 2.8.

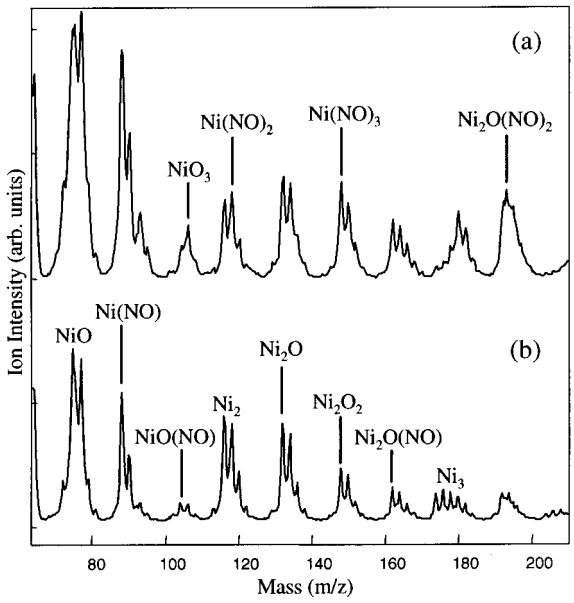

Figure 3. Comparison of product distributions for the reaction $Ni_x^+ + NO$ at (a) 2 sccm and (b) 1 sccm of NO.

There is a tendency toward higher oxygen content with dimer and trimer species as in the case of $Ni_2O_5^+$, $Ni_3O_6^+$, $Ni_3O_6^-$, $Ni_2O_5^-$, and $Ni_2O_4^-$. This could be explained by excess weakly bonded O_2 as has been seen for smaller vanadium clusters.[10] It is also worth noting that no nickel-rich oxides are formed when there is excess oxygen present, which is to be expected since nickel-rich clusters would have oxidation states less than 2.

Nickel Cluster Cation Reactions. Nitric oxide was reacted with nickel cluster cation distributions such as the one shown in Figure 1. These reactions produced two main types of products, oxidation of the nickel clusters and addition of nitric oxide to both the nickel and newly formed nickel oxide clusters. Figure 3 shows the low-mass product species at 1 sccm (bottom spectrum) and 2 sccm (top spectrum) of nitric oxide. The species just to the left of each spectrum, but not fully shown, is the nickel monomer. No product species having masses less than that of the monomer were observed in the study. The first product above the monomer is NiO^+. While there was a small amount of NiO^+ in the initial reactant distribution, it increased more than an order of magnitude upon adding NO. Other oxidation products are also labeled in Figure 3, such as NiO_3^+, Ni_2O^+, and $Ni_2O_2^+$.

Clusters with additions of NO are the second type of major products seen in the reaction distributions. Nickel monomer is observed to form both $Ni(NO)^+$ and $Ni(NO)_2^+$, and possibly $Ni(NO)_3^+$. $Ni(NO)_3^+$ overlaps with Ni_2O_2, so it is difficult to determine how much, if any, of this addition product is formed. Also a small amount of $NiO(NO)^+$ species is formed. The dimer produces only nickel oxide addition species, and no addition of NO is observed with bare nickel dimer. The addition products observed for nickel dimer oxides are $Ni_2O(NO)^+$, $Ni_2O(NO)_2^+$, and $Ni_2O(NO)_3^+$. The latter product is shown in Figure 4 along with other cluster species that become very prominent in the spectra at 2 sccm of nitric oxide. These become magic peaks at 10 sccm, which indicates species of unusually high stability. The 2, 1, 3 ($Ni_2O(NO)_3^+$) and 3, 1, 3 ($Ni_3O(NO)_3^+$) could be considered magic at both concentrations. The increase in NO concentration to 10 sccm (Figure 4a) from 2 sccm (Figure 4b) causes only a slight shift toward the 3, 1, 3 species. At concentrations above 2 sccm, the 4, 2, 3 begins to decrease, indicating only a moderate stability compared with other magic

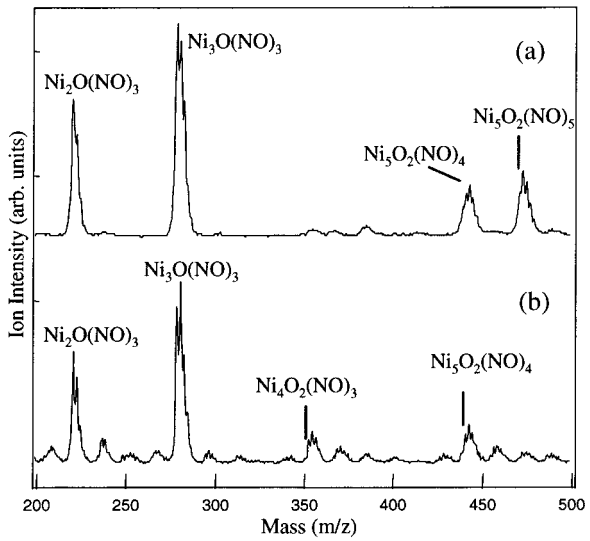

Figure 4. Spectra displaying the appearance of magic peaks for the reaction $Ni_x^+ + NO$ at (a) 10 sccm and (b) 2 sccm of NO.

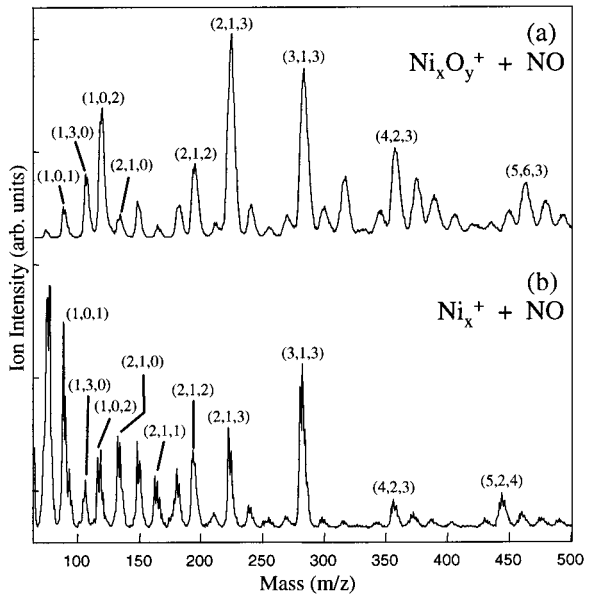

Figure 5. Comparison of the reaction of (a) the nickel oxide clusters and (b) the bare nickel clusters with NO at 2 sccm. The species $Ni_xO_y(NO)_z^+$ are labeled as (*x*, *y*, *z*). These spectra show the similarity in reaction products formed.

peaks. Also, as the concentration increases, the 5, 2, 4 feeds into the more stable or preferred 5, 2, 5 species.

Many of the species that lead up to the more stable species can be seen at lower concentrations. However, there is no obvious or traceable single buildup pattern that can be determined from the species at lower concentration, and it appears that there may be more than one buildup pattern occurring.

Nickel Oxide Cluster Cation Reactions. Nickel oxide cluster distributions such as the one shown in Figure 2 were also reacted with nitric oxide. A surprising result from these reactions can be seen when these product distributions are compared with product distributions for the reactions of nitric oxide with bare nickel clusters. Figure 5 shows this comparison, where the product distribution for $Ni_xO_y^+ + NO$ is shown in the top spectrum and the product distribution for $Ni_x^+ + NO$ is given in the bottom spectrum; both distributions are obtained at 2 sccm of NO. The most noticeable similarity is seen in the two lower mass magic number species discussed previously, namely, the 2, 1, 3 and the 3, 1, 3. Again, these species are found to be the most stable form of mixed nickel/nitric oxide clusters for the dimer and trimer species. There are many more similarities between the product distributions. The third magic number discussed above, namely, 4, 2, 3, is also a quite prominent product species in the reaction of nitric oxide with nickel oxides. In fact, a careful comparison of the two product distributions in Figure 5 shows that, with the exception of the 2, 1, 1 species in the lower spectrum ($Ni_x^+ + NO$), every peak found in the low-mass region (under 300 amu) is the same in both distributions. This species, the 2, 1, 1, is however seen at lower concentrations (0.5 sccm) of nitric oxide in the $Ni_xO_y^+ + NO$ reactions. The species labeled in each distribution are the only possible products at each particular mass. Those not labeled in Figure 5 have more than one possible mass assignment, and although each corresponds to the same mass in each spectrum, they may still be different products. For example, the three unlabeled peaks to the left of the 2, 1, 3 species are at masses 148, 180, and 210 amu (masses are given for the first isotope). The 148-amu peak could either be $Ni_2O_2^+$ or $Ni(NO)_3^+$ and may not be the same species in each of the two distributions. The 180-amu peak could be either $Ni_2O_3^+$ or $NiO(NO)_3^+$ and the peak at 210 amu could be $Ni_2O_3(NO)^+$ or $NiO(NO)_4^+$. However, regarding the three possible alternatives listed above, the isotope patterns best fit the nickel dimer, indicating that they are likely to be the same products in the upper and lower spectra. As the concentration is increased, the $Ni_xO_y^+ + NO$ reactions yield significantly different species. Exceptions are the 3, 1, 3 species, which remains the most prominent of all clusters, and the 2, 1, 3, which is still a significant product at 10 sccm of NO.

Although there is evidence for a simple addition process, it cannot fully explain all of the species observed in the product distributions. The disappearance of the tetramer species at higher concentrations can only be explained by some type of fragmentation process. Additionally, there is insufficient trimer starting material (Ni_3O_3 and Ni_3O_4) to produce the large amount of $Ni_3O(NO)_3$ observed in the product distributions. Furthermore, some other mechanistic processes must be considered in order to explain the similarity found in the two different reactions.

A careful examination of the various reaction products at different concentrations suggests that there may be many different reaction mechanisms occurring. However, without the ability to follow individual reactants through their reaction channels it is often difficult, if not impossible, to elucidate specific reaction mechanisms. Under such conditions where a complicated mixture of different reaction mechanisms is occurring, careful consideration must be made to determine what exactly can be unambiguously shown to be occurring. The first steps to a replacement type mechanism can be seen in Figure 6. This figure illustrates that NO adds to the cluster and the process of bonding to the cluster causes the loss of oxygen from the cluster. The data presented in the figure suggests the addition of NO to the nickel oxide starting material (bottom spectrum) by the diagonal lines. It is not known in what form oxygen is removed from the cluster, although one reasonable pathway for this to occur may be that oxygen is extracted from the cluster by a second NO molecule in the form of NO_2.

Kinetic Data. Kinetic investigations of nickel cluster cation reactions with both O_2 and NO, as well as reactions of nickel oxides with NO, were performed. Determination of the pseudo-first-order bimolecular rate constants for the reactions

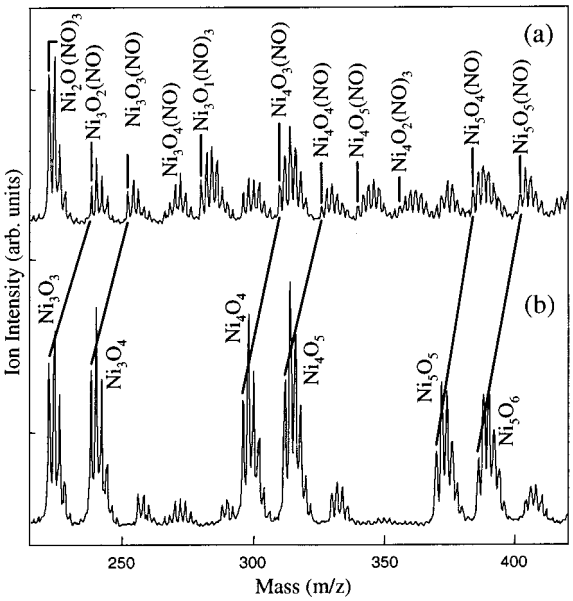

Figure 6. Product distribution for (a) the reaction $Ni_xO_y^+ + NO$ at 2 sccm and the mass distribution (b) for $Ni_xO_y^+$, clearly indicating the oxygen loss channel.

$$Ni_x^+ + NO \rightarrow\rightarrow Ni_xO_y(NO)_z^+ + \text{neutrals} \quad (1a)$$

$$Ni_xO_y^+ + NO \rightarrow\rightarrow Ni_xO_y(NO)_z^+ + \text{neutrals} \quad (1b)$$

are obtained from the slope of semilog plots through the relation

$$\ln(I/I_0) = -k[NO]t \quad (2)$$

where I/I_0 is the intensity of the Ni_x^+ or $Ni_xO_y^+$ reactant clusters, respectively, at given concentrations of NO divided by the intensity of these same species at zero concentration of the NO reactant, k is the rate constant, and t is the reaction time (4.2 ms measured by pulsing experiments[11]). Examples of the semilog plots used to determine rate constants for each of the reactions carried out in these experiments are given in Figure 7.

The rate constants for these reactions are given in Tables 1−3 and are determined by averaging several different data sets in order to reduce the effect of scan-to-scan fluctuations in the data. Some reaction products overlap with starting material, but often these reaction rates could be obtained from starting material isotopes that did not overlap and these are the ones reported here. Reaction rates for NO reactions were often quite difficult to obtain because many of the major peaks in the isotope patterns of nickel are exactly 60 amu apart (2 NO is 60 amu). To over come this problem, high-resolution spectra were obtained so that the first isotopes of the nickel clusters (58 amu apart) could be used to differentiate reactants from products. The need to collect data at higher resolution for NO reactions compared with O_2 reactions resulted in the determination of NO reaction rates for nickel and nickel oxides up to cluster sizes of 8 nickels compared to 16 nickels for O_2 reactions. Sufficient signal intensity is needed for the determination of reaction rates, and increasing resolution dramatically reduces signal intensity. All reaction rates that could be obtained without interference from reactant and product overlap are reported in Tables 1−3 and are given in cm^3/s. The larger errors reported in some reaction rates are attributable to the eventual overlap of reactants with products at increasing degrees of reaction. This acts to reduce usable data points. Also, lower concentrations of starting

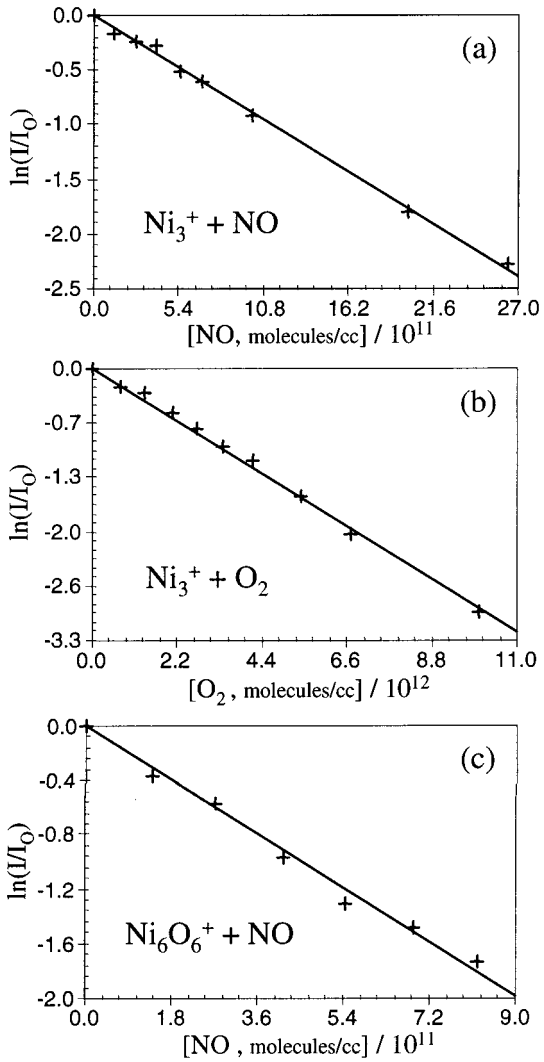

Figure 7. Examples of semilog plots for rate constant determination for (a) $Ni_3^+ + NO$, (b) $NI_3^+ + O_2$, and (c) $Ni_6O_6^+ + NO$.

TABLE 1: Rate Constants for the Reactions of Nickel Cluster Cations with NO

reaction	experimental rate constants (10^{-10} cm^3 s^{-1})	calculated collision rates (10^{-9} cm^3 s^{-1})
$Ni_2^+ + NO \rightarrow\rightarrow Ni_2O_x(NO)_y^+$	1.15 ± 0.15	1.55
$Ni_3^+ + NO \rightarrow\rightarrow Ni_3O_x(NO)_y^+$	2.07 ± 0.18	1.55
$Ni_4^+ + NO \rightarrow\rightarrow Ni_4O_x(NO)_y^+$	7.9 ± 0.8	1.52
$Ni_5^+ + NO \rightarrow\rightarrow Ni_5O_x(NO)_y^+$	8.3 ± 0.8	1.51
$Ni_6^+ + NO \rightarrow\rightarrow Ni_6O_x(NO)_y^+$	6.7 ± 0.9	1.49
$Ni_7^+ + NO \rightarrow\rightarrow Ni_7O_x(NO)_y^+$	7.1 ± 0.9	1.49
$Ni_8^+ + NO \rightarrow\rightarrow Ni_8O_x(NO)_y^+$	4.7 ± 0.9	1.48

material of the larger clusters contributed to these errors. In addition to reaction rates, calculated collision rates (Langevin limit for nonpolar molecules and Su−Chesnavich parametrization for polar molecules)[12] are provided in each table. A comparison of these collision rates with the experimentally determined rates gives an indication of the efficiency of the reactions. The reaction rates of nitric oxide reaction with nickel cluster cations are given in Table 1.

It is interesting to compare the reaction rates in Table 1 with those of oxygen with nickel cluster cations in Table 2. Also reaction rates for nickel oxide cluster cations with nitric oxide are given in Table 3, where again only those reaction rates that are not obscured by product overlap are listed. The reaction rates for both nickel and nickel oxide with nitric oxide are

TABLE 2: Rate Constants for the Reaction of Bare Nickel Cluster Cations with Molecular Oxygen

reaction	experimental rate constants (10^{-11} cm^3 s^{-1})	calculated collision rates (10^{-10} cm^3 s^{-1})	nickel *anion* rate constants[4] (10^{-10} cm^3 s^{-1})
$Ni_3^+ + O_2 \rightarrow Ni_3O_x^+$	6.9 ± 0.7	5.66	1.12 ± 0.08
$Ni_4^+ + O_2 \rightarrow Ni_4O_x^+$	7.1 ± 0.7	5.55	3.01 ± 0.43
$Ni_5^+ + O_2 \rightarrow Ni_5O_x^+$	6.9 ± 0.3	5.48	2.98 ± 0.15
$Ni_6^+ + O_2 \rightarrow Ni_6O_x^+$	7.9 ± 0.4	5.43	1.91 ± 0.16
$Ni_7^+ + O_2 \rightarrow Ni_7O_x^+$	7.2 ± 0.7	5.40	2.53 ± 0.28
$Ni_8^+ + O_2 \rightarrow Ni_8O_x^+$	6.7 ± 1.0	5.38	2.49 ± 0.26
$Ni_9^+ + O_2 \rightarrow Ni_9O_x^+$	7.3 ± 0.3	5.36	2.44 ± 0.18
$Ni_{10}^+ + O_2 \rightarrow Ni_{10}O_x^+$	7.7 ± 0.9	5.34	3.19 ± 0.45
$Ni_{11}^+ + O_2 \rightarrow Ni_{11}O_x^+$	7.4 ± 1.2	5.33	4.39 ± 0.36
$Ni_{12}^+ + O_2 \rightarrow Ni_{12}O_x^+$	6.7 ± 1.3	5.32	4.06 ± 0.38
$Ni_{13}^+ + O_2 \rightarrow Ni_{13}O_x^+$	7.1 ± 1.1	5.31	4.12 ± 0.26
$Ni_{14}^+ + O_2 \rightarrow Ni_{14}O_x^+$	6.6 ± 1.5	5.30	2.4 ± 0.7
$Ni_{15}^+ + O_2 \rightarrow Ni_{15}O_x^+$	7.7 ± 0.9	5.30	2.7 ± 1.0
$Ni_{16}^+ + O_2 \rightarrow Ni_{16}O_x^+$	6.0 ± 1.5	5.29	

TABLE 3: Rate Constants for the Reaction of Nickel Oxide Cluster Cations with NO

reaction	experimental rate constants (10^{-10} cm^3 s^{-1})	calculated collision rates (10^{-9} cm^3 s^{-1})
$Ni_2O_5^+ + NO \rightarrow Ni_xO_y(NO)_z^+$	5.8 ± 1.3	1.54
$Ni_3O_3^+ + NO \rightarrow Ni_xO_y(NO)_z^+$	1.4 ± 0.4	1.53
$Ni_4O_4^+ + NO \rightarrow Ni_xO_y(NO)_z^+$	2.8 ± 0.7	1.50
$Ni_4O_5^+ + NO \rightarrow Ni_xO_y(NO)_z^+$	8.6 ± 2.1	1.50
$Ni_5O_5^+ + NO \rightarrow Ni_xO_y(NO)_z^+$	8.2 ± 1.0	1.49
$Ni_6O_6^+ + NO \rightarrow Ni_xO_y(NO)_z^+$	5.3 ± 0.9	1.49
$Ni_7O_8^+ + NO \rightarrow Ni_xO_y(NO)_z^+$	5.6 ± 0.8	1.48
$Ni_8O_{10}^+ + NO \rightarrow Ni_xO_y(NO)_z^+$	5.4 ± 1.3	1.48

considerably faster than the reaction rates for oxygen with nickel cation clusters. Also, the reactions of oxygen with nickel anion clusters are considerably faster than the same reactions with nickel cations. These considerably slower rates are consistent with what is observed in the product distributions. For instance, as previously discussed, nickel cation clusters appear to saturate with oxygen more slowly than do anion clusters.

IV. Conclusion

The reactions of nitric oxide with nickel and nickel oxide cluster cations are presented. Pseudo-first-order bimolecular rate constants for these reactions and the reactions of O_2 with nickel cluster cations are also reported. The product distributions indicate that several different reaction mechanisms occur between NO and Ni_x and $Ni_xO_y^+$. Competing processes such as oxidation, NO addition, and replacement of oxygen with nitric oxide are observed to occur. Also, the presence of magic peaks in the distributions indicates unusually stable product cluster species. The similarities in the low-mass region of the product distributions for the reactions of nitric oxide with both nickel and nickel oxide cluster cations further demonstrate the unusual stability of the $Ni_3O(NO)_3^+$ cluster and, to a slightly lesser degree, the $Ni_2O(NO)_3^+$ cluster.

Acknowledgment. Funding provided by the Department of Energy, Grant DE-FG02-92ER14258, is gratefully acknowledged.

References and Notes

(1) (a) Riley, S. E. In *Metal Ligand Interactions*: *From Atoms, to Clusters, to Surfaces*; Salahub, D. R., Russo, N., Eds.; Kluwer Academic Press: Dordrecht, 1992; pp 17−36. (b) Eller, K.; Schwarz, H. *Chem. Rev.* **1991**, *91*, 1121.

(2) (a) Fialko, E. F.; Kikhtenko, A. V.; Goncharov, V. B.; Zararaev, K. I. *J. Phys. Chem.* **1997**, *101*, 5772. (b) Shröder, D.; Schwarz, H. *Angew. Chem., Int. Ed. Engl.* **1995**, *34*, 1973.

(3) Vann, W. D.; Wagner, R. L.; Castleman, A. W., Jr. *J. Phys. Chem. A* **1998**, *102*, 1708.

(4) Vann, W. D.; Wagner, R. L.; Castleman, A. W., Jr. *J. Phys. Chem. A* **1998**, *102*, 8804.

(5) Castleman, A. W., Jr.; Weil, K. G.; Sigsworth, S. W.; Leuchtner, R. E.; Keesee, R. G. *J. Chem. Phys.* **1987**, *86*, 3829.

(6) Cotton, F. A.; Wilkinson, G. *Advanced Inorganic Chemistry, a Comprehensive Text*, 3rd ed.; John Wiley & Sons, Inc.: New York, 1972.

(7) Kim, K. S.; Winograd, N. *Surf. Sci.* **1974**, *43*, 625.

(8) Wells, A. F. *Structural Inorganic Chemistry*, 5th ed.; Oxford University Press: New York, 1991; p 538.

(9) (a) Greenwood, N. N.; Earnshaw, A. *Chemistry of the Elements*; Pergamon Press: Oxford, 1984. (b) *CRC Handbook of Chemistry and Physics*, 76th ed.; Lide, D. R., Ed.; CRC Press, Inc.: Boca Raton, FL, 1996.

(10) Bell, R. C.; Zemski, K. A.; Kerns, K. P.; Deng, H. T.; Castleman, A. W., Jr. *J. Phys. Chem. A* **1998**, *102*, 1733.

(11) (a) Pulsing experiments are conducted by interrupting a continuous signal with an electrical pulse at the reactant gas inlet and the sampling orifice. The time difference measured between these two interruptions is the residence time of ions in the reaction zone, under those experimental conditions. (b) MacTaylor, R. S.; Vann, W. D.; Castleman, A. W., Jr. *J. Phys. Chem.* **1996**, *100*, 5329.

(12) Mackay, G. I.; Betowski, L. D.; Payzant, J. D.; Schiff, H. I.; Bohme, D. K. *J. Phys. Chem.* **1976**, *80*, 2919. Su, T.; Chesnavich, W. J. *J. Chem. Phys.* **1982**, *76*, 5183.

(13) (a) Nayak, S. K.; Khanna, S. N.; Rao, B. K.; Jena, P. *J. Phys. Chem. A* **1997**, *101*, 1072. (b) Stave, M. S.; DePristo, A. E. *J. Chem. Phys.* **1992**, *97*, 3386.